

WKB Analysis of the Scattering of Massive Dirac Fields in Schwarzschild Black Hole Spacetimes

H. T. Cho* and Y.-C. Lin

*Department of Physics, Tamkang University,
Tamsui, Taipei, Taiwan, Republic of China*

(Dated: June 14, 2021)

Abstract

We analysis the radial equations for massive Dirac fields in Schwarzschild black hole spacetimes. Different approximation formulae under the WKB scheme are developed for the transmission probability \mathcal{T} of the radial wavefunction with $E^2 \gg V_m$, $E^2 \approx V_m$, and $E^2 \ll V_m$, where E is the energy of the field and V_m is the maximum value of the effective potential. Explicit results of \mathcal{T} in these approximations are given for various values of E , the mass m , and the angular momentum parameter κ of the fields. We also discuss the dependence of \mathcal{T} on these parameters.

arXiv:gr-qc/0411090v1 18 Nov 2004

*Electronic address: htcho@mail.tku.edu.tw

I. INTRODUCTION

One of the most useful and efficient ways to study the properties of black holes is by scattering matter waves off them [1]. From the more practical point of view, the study of wave scattering in black hole spacetimes is crucial to the understanding of the signals expected to be received by the new generation of gravitational-wave detectors in the near future [2]. Since the linear perturbations of black holes are represented by fields of integral spins, the study of the scattering of wave fields are concentrated on these cases while that of the Dirac fields are thus less common, especially for the massive ones [1, 3]. Recently, Finster and collaborators [4] have renewed the interests in that of the massive Dirac fields by investigating in details their evolutions in various black hole spacetimes. Here we would like to work in this direction by considering the scattering solutions of the radial equations of massive Dirac fields in spherically symmetric Schwarzschild black hole spacetimes.

There are both numerical and analytical methods in solving the various wave equations in black hole scattering [1]. In this work we shall use the semi-analytic WKB approximation [5, 6], which has been proven to be very useful and accurate in many cases like, for example, the evaluation of the quasinormal mode frequencies [7, 8]. For the radial Dirac equations we consider here, the effective potential can change from a barrier to a step and vice versa when the mass m or the angular momentum parameter κ are varied. The WKB scheme can be accommodated in various ways to consider all these situations with different values of the energy E of the field, whether it is above or below the maximum value V_m of the potential.

In [9], Mukhopadhyay and Chakrabarti have studied in details the radial equations of a massive Dirac field in the Schwarzschild black hole spacetime using a modified WKB (they called it the "instantaneous WKB") approximation. However, they only looked at the case with $m = M/2$, where M is the mass of the black hole, $\kappa = 1$, and $E \approx m$. In this paper we use the standard WKB scheme instead, and we shall extend the consideration to cases with different values of m and κ . In addition, we shall consider all possible values of E with $E \geq m$. In this manner we can discuss the variations of the transmission probabilities with respect to these various parameters.

In the next section, we consider the reduction of the massive Dirac equation in Schwarzschild spacetimes into a set of Schrödinger-like equations. We also discuss briefly the properties of the corresponding effective potential [10]. In Section III, we look at the

three different WKB schemes for the cases with $E^2 \gg V_m$, $E^2 \approx V_m$, and $E^2 \ll V_m$. Explicit approximated formulae for the transmission probability are given. In Section IV, we apply the formulation to calculate the transmission probabilities of the massive radial Dirac equations for various values of E , m , and κ . Conclusions and discussions are given in Section V.

II. DIRAC EQUATION IN THE SCHWARZSCHILD SPACETIME

In this section we discuss briefly the massive Dirac equation in the Schwarzschild black hole spacetime, including its reduction to a set of Schrödinger-like radial equations and the properties of the corresponding effective potentials.

A. Radial equations

In the Schwarzschild spacetime,

$$ds^2 = -\frac{\Delta}{r^2} dt^2 + \frac{r^2}{\Delta} dr^2 + r^2 d\theta^2 + r^2 \sin^2\theta d\phi^2, \quad (1)$$

where $\Delta = r(r - 2M)$ and M is the mass of the black hole. Consider the Dirac equation in this background spacetime [11],

$$[\gamma^a e_a^\mu (\partial_\mu + \Gamma_\mu) + m]\Psi = 0, \quad (2)$$

where m is the mass of the Dirac field, and e_a^μ is the inverse of the vierbein e_μ^a defined by the metric $g_{\mu\nu}$,

$$g_{\mu\nu} = \eta_{ab} e_\mu^a e_\nu^b, \quad (3)$$

with $\eta_{ab} = \text{diag}(-1, 1, 1, 1)$ being the Minkowski metric. γ^a are the Dirac matrices

$$\gamma^0 = \begin{pmatrix} -i & 0 \\ 0 & i \end{pmatrix}, \quad \gamma^i = \begin{pmatrix} 0 & -i\sigma^i \\ i\sigma^i & 0 \end{pmatrix}, \quad i = 1, 2, 3, \quad (4)$$

where σ^i are the Pauli matrices. Γ_μ is the spin connection given by

$$\Gamma_\mu = \frac{1}{8} [\gamma^a, \gamma^b] e_a^\nu e_{b\nu;\mu}, \quad (5)$$

where $e_{b\nu;\mu} = \partial_\mu e_{b\nu} - \Gamma_{\mu\nu}^\alpha e_{b\alpha}$ is the covariant derivative of $e_{b\nu}$ with $\Gamma_{\mu\nu}^\alpha$ being the Christoffel symbols.

Here it is convenient to choose the vierbein

$$e_{\mu}^a = \begin{pmatrix} \Delta^{1/2}/r & 0 & 0 & 0 \\ 0 & r\sin\theta \cos\phi/\Delta^{1/2} & r\sin\theta \sin\phi/\Delta^{1/2} & r\cos\theta/\Delta^{1/2} \\ 0 & r\cos\theta \cos\phi & r\cos\theta \sin\phi & -r\sin\theta \\ 0 & -r\sin\theta \sin\phi & r\sin\theta \cos\phi & 0 \end{pmatrix}. \quad (6)$$

Since the spacetime is spherically symmetric, one can, after some algebra, simplify the Dirac equation to [11, 12]

$$\frac{\gamma^0 r}{\Delta^{1/2}} \frac{\partial \Psi}{\partial t} + \frac{\tilde{\gamma} \Delta^{1/4}}{r^{3/2}} \frac{\partial}{\partial r} (r^{1/2} \Delta^{1/4} \Psi) - \frac{\tilde{\gamma}}{r} (\vec{\Sigma} \cdot \vec{L} + 1) \Psi + m \Psi = 0, \quad (7)$$

where $\tilde{\gamma}$ is defined as

$$\tilde{\gamma} = \gamma^1 \sin\theta \cos\phi + \gamma^2 \sin\theta \sin\phi + \gamma^3 \cos\theta. \quad (8)$$

Also

$$\vec{\Sigma} = \begin{pmatrix} \vec{\sigma} & 0 \\ 0 & \vec{\sigma} \end{pmatrix}, \quad (9)$$

and $\vec{L} = \vec{r} \times \vec{p}$ are the ordinary angular momentum operators. The wavefunction Ψ can be separated into its radial and angular parts by writing

$$\Psi = \frac{1}{r^{1/2} \Delta^{1/4}} e^{-iEt} \Phi, \quad (10)$$

where [13]

$$\Phi(r, \theta, \phi) = \begin{pmatrix} \frac{iG^{(\pm)}(r)}{r} \varphi_{jm}^{(\pm)}(\theta, \phi) \\ \frac{F^{(\pm)}(r)}{r} \varphi_{jm}^{(\mp)}(\theta, \phi) \end{pmatrix}, \quad (11)$$

with the angular parts of the wavefunction

$$\varphi_{jm}^{(+)} = \begin{pmatrix} \sqrt{\frac{l+1/2+m}{2l+1}} Y_l^{m-1/2} \\ \sqrt{\frac{l+1/2-m}{2l+1}} Y_l^{m+1/2} \end{pmatrix}, \quad (12)$$

for $j = l + 1/2$, and

$$\varphi_{jm}^{(-)} = \begin{pmatrix} \sqrt{\frac{l+1/2-m}{2l+1}} Y_l^{m-1/2} \\ -\sqrt{\frac{l+1/2+m}{2l+1}} Y_l^{m+1/2} \end{pmatrix}, \quad (13)$$

for $j = l - 1/2$.

Then the radial equations [10, 14] can be written as

$$\left(-\frac{d^2}{dx^2} + V_1 \right) \hat{F} = E^2 \hat{F}, \quad (14)$$

$$\left(-\frac{d^2}{dx^2} + V_2 \right) \hat{G} = E^2 \hat{G}, \quad (15)$$

where

$$V_{1,2} = \pm \frac{dW}{dx} + W^2, \quad (16)$$

with

$$W = \frac{\Delta^{1/2}(\kappa^2 + m^2 r^2)^{3/2}}{r^2(\kappa^2 + m^2 r^2) + m\kappa\Delta/2E}, \quad (17)$$

where

$$x = r + 2M \ln \left(\frac{r}{2M} - 1 \right) + \frac{1}{2E} \tan^{-1} \left(\frac{mr}{\kappa} \right). \quad (18)$$

Here we have combined the (+) and the (-) cases, with κ going over all positive and negative integers. Positive integers represent the (+) cases with

$$\kappa = j + \frac{1}{2} \quad \text{and} \quad j = l + \frac{1}{2}, \quad (19)$$

and

$$\begin{pmatrix} \hat{F} \\ \hat{G} \end{pmatrix} = \begin{pmatrix} \sin(\theta/2) & \cos(\theta/2) \\ \cos(\theta/2) & -\sin(\theta/2) \end{pmatrix} \begin{pmatrix} F \\ G \end{pmatrix}, \quad (20)$$

where

$$\theta = \tan^{-1}(mr/\kappa). \quad (21)$$

While negative integers represent the (-) cases with

$$\kappa = - \left(j + \frac{1}{2} \right) \quad \text{and} \quad j = l - \frac{1}{2}, \quad (22)$$

and

$$\begin{pmatrix} \hat{F} \\ \hat{G} \end{pmatrix} = \begin{pmatrix} \cos(\theta/2) & -\sin(\theta/2) \\ \sin(\theta/2) & \cos(\theta/2) \end{pmatrix} \begin{pmatrix} F \\ G \end{pmatrix}. \quad (23)$$

From the Schrödinger-like equations in Eqs. (14) and (15), we shall consider the scattering of the massive Dirac fields. Note that V_1 and V_2 , which are related as shown in Eq. (16), are supersymmetric partners derived from the same superpotential W [15]. It has been shown that potentials related in this way possess the same spectra, discrete as well as continuous [16]. Physically this just indicates that Dirac particles and antiparticles will scatter in the same manner around the Schwarzschild black hole. We shall therefore concentrate just on Eq. (14) with potential V_1 in the following sections.

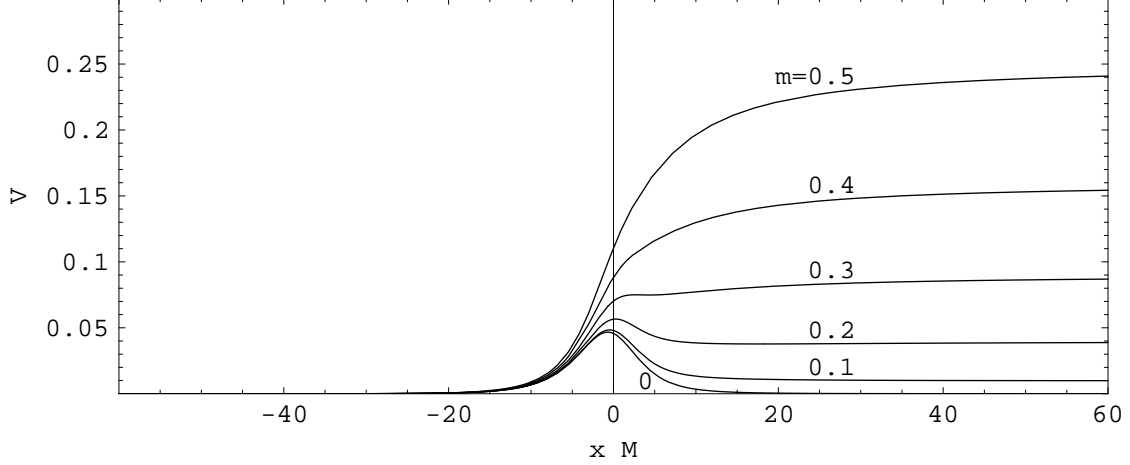


FIG. 1: Variation of the effective potential with the mass m (in units of M) of the Dirac field for $\kappa = 1$ and $E = M$.

B. Properties of the effective potential

Here we discuss briefly the dependence of the effective potential

$$\begin{aligned}
 & V(r, \kappa, m, E) \\
 = & \frac{\Delta^{1/2}(\kappa^2 + m^2 r^2)^{3/2}}{(r^2(\kappa^2 + m^2 r^2) + m\kappa\Delta/2E)^2} \left[\Delta^{1/2}(\kappa^2 + m^2 r^2)^{3/2} + ((r-1)(\kappa^2 + m^2 r^2) + 3m^2 r\Delta) \right] \\
 & - \frac{\Delta^{3/2}(\kappa^2 + m^2 r^2)^{5/2}}{(r^2(\kappa^2 + m^2 r^2) + m\kappa\Delta/2E)^3} \left[2r(\kappa^2 + m^2 r^2) + 2m^2 r^3 + m\kappa(r-1)/E \right]. \quad (24)
 \end{aligned}$$

on the parameters m , κ , and E . Since we shall only work with V_1 , but not V_2 , we have dropped the subscript of V .

First, its dependence on m is showed in Fig. 1 with energy $E = M$ and with $\kappa = 1$. Note that we have shown V as a function of x in the figure. For small values of m , the potential is in the form of a barrier, with the asymptotic value

$$V(x \rightarrow \infty) = m^2. \quad (25)$$

As m is increased, the peak of the potential also increases but does so very slowly. Eventually, the height of the peak is lower than the asymptotic value m^2 . When m is increased further, the peak disappears altogether, and the potential barrier turns effectively into a potential step.

The effective potential V also depends on the energy E . However, as shown in [10], the general behaviors of the potential remain the same as E is increased from its minimum value

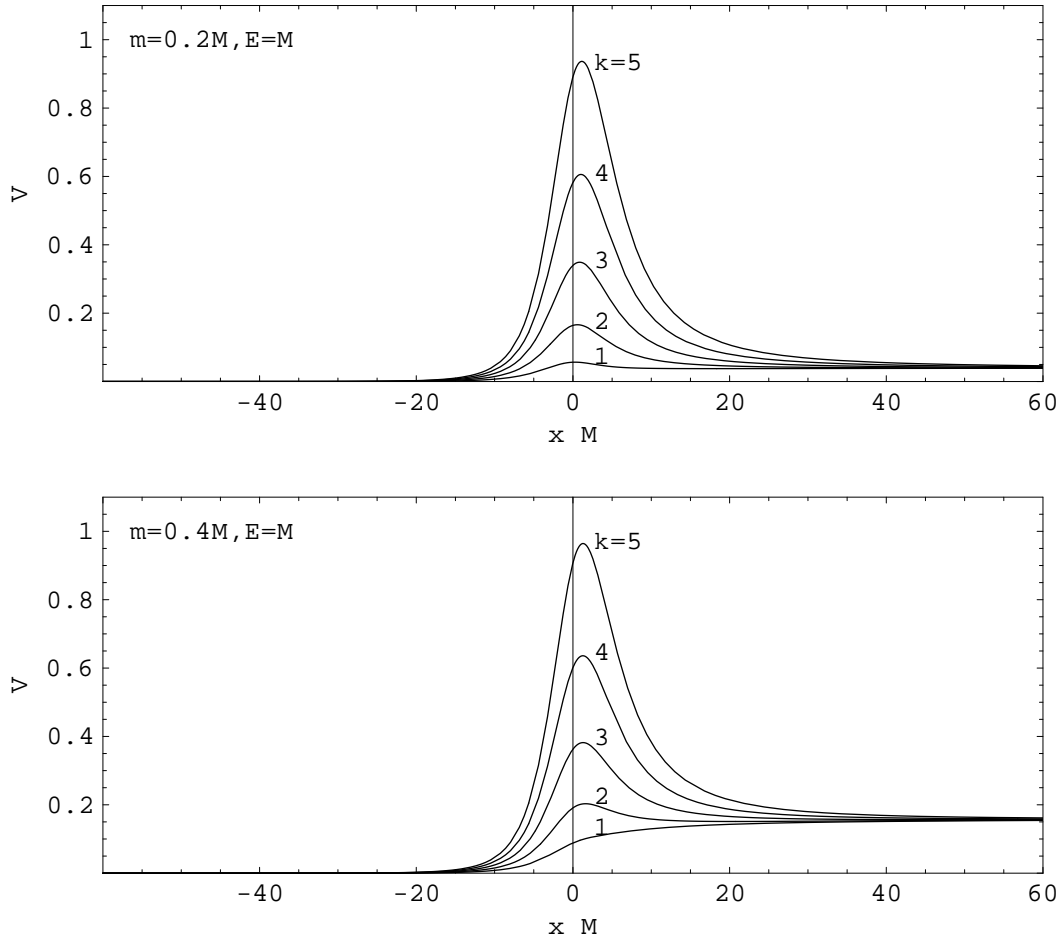


FIG. 2: Variation of the effective potential with κ for the Dirac fields of $m = 0.2M$ and $0.4M$.

m . Indeed, from the form of the potential in Eq. (24), E appears all in the denominators. The terms involving E can never get large enough to change the general behaviors of the potential since E cannot be smaller than m .

Finally, in Fig. 2 we show the dependence of the effective potential with the angular momentum quantum number κ . We see that as κ increases, the behaviors of the potential approach to that of the massless one, regardless of the mass of the field. This can be seen by taking the limit $|\kappa| \rightarrow \infty$ in Eq. (24),

$$V(|\kappa| \rightarrow \infty) \approx \frac{\Delta \kappa^2}{r^4}, \quad (26)$$

which is independent of m .

III. WKB APPROXIMATIONS

In this section we consider the radial equations obtained in the previous section as a general one-dimensional quantum mechanical problem,

$$\left(-\frac{d^2}{dx^2} + V\right)\psi = E^2\psi, \quad (27)$$

with the asymptotic values of the potential

$$V(x \rightarrow \infty) = m^2 \quad \text{and} \quad V(x \rightarrow -\infty) = 0. \quad (28)$$

Suppose an incident wave comes from the right ($x = \infty$). Then the boundary conditions for ψ are

$$\psi(x \rightarrow \infty) = e^{-i\sqrt{E^2-m^2}x} + Re^{i\sqrt{E^2-m^2}x} \quad (29)$$

$$\psi(x \rightarrow -\infty) = Te^{-iEx}, \quad (30)$$

where R and T represent the reflection and transmission coefficients, respectively.

Since exact solutions for Eq. (27) are usually hard to find, we have to resort to approximations. Here we adopt the WKB approximation, which has been proved to be extremely useful and sometimes to be more accurate than expected. We try to develop approximate expressions for the transmission probability

$$\mathcal{T} = \sqrt{\frac{E^2}{E^2 - m^2}} |T|^2, \quad (31)$$

for the whole range of the energy E , including the cases with $E^2 \gg V_m$, $E^2 \approx V_m$, and $E^2 \ll V_m$, where V_m is the maximum value of the potential. In the case of a barrier, V_m will be the peak value of V , while in the case of a step, $V_m = m^2$.

A. $E^2 \gg V_m$

For $E^2 \gg V_m$, the standard WKB form of the wavefunction can be given by

$$\psi(x) = C_+W_+(x) + C_-W_-(x), \quad (32)$$

for $-\infty < x < \infty$, with

$$W_{\pm}(x) = \frac{1}{\sqrt{p(x)}} e^{\pm i \int_{x_0}^x dx' p(x')} \quad (33)$$

being the WKB wavefunctions. Here $p(x) = \sqrt{E^2 - V(x)}$, x_0 is some fixed reference point, and C_+ and C_- are constants to be determined from the boundary conditions. Eq. (32) is a useful approximation for the wavefunction as long as the validity condition

$$\left| \frac{V'}{2p^3} \right| \ll 1, \quad (34)$$

where $V' = dV/dx$, is fulfilled.

From the boundary condition at $x \rightarrow -\infty$ (Eq. (30)), we have $C_+ = 0$, while from the condition at $x \rightarrow \infty$ (Eq. (29)), we have

$$C_- = (E^2 - m^2)^{1/4} e^{-i\sqrt{E^2 - m^2} x_0} e^{i \int_{x_0}^{\infty} dx' (p(x') - \sqrt{E^2 - m^2})}. \quad (35)$$

Therefore, the transmission coefficient

$$\begin{aligned} T &= \frac{C_-}{\sqrt{E}} e^{iEx_0} e^{i \int_{-\infty}^{x_0} dx' (p(x') - E)} \\ &= \left(\frac{E^2 - m^2}{E^2} \right)^{1/4} e^{i(E - \sqrt{E^2 - m^2})x_0} e^{i \int_{x_0}^{\infty} dx' (p(x') - \sqrt{E^2 - m^2})} e^{i \int_{-\infty}^{x_0} dx' (p(x') - E)}, \end{aligned} \quad (36)$$

and the transmission probability in Eq. (31) becomes

$$\mathcal{T} = 1. \quad (37)$$

This is of course consistent with the classical result in which the particle moves to the left without rebounding. However, quantum mechanically \mathcal{T} is not exactly equal to 1, there is always a small probability for reflection. Thus to get a better approximation on \mathcal{T} in this quantum mechanical situation, we need to extend the WKB scheme used here.

Suppose we write the general solution of Eq. (27) as [5]

$$\psi = C_+(x)W_+(x) + C_-(x)W_-(x), \quad (38)$$

where $C_+(x)$ and $C_-(x)$ are now functions of x . If we also take

$$C'_+(x)W_+(x) + C'_-(x)W_-(x) = 0, \quad (39)$$

and together with Eq. (38), we can obtain the differential equations for C_{\pm} ,

$$C'_{\pm}(x) = \mp i \left(\frac{p''(x)}{4p(x)^2} - \frac{3(p'(x))^2}{8p(x)^3} \right) \left[C_{\pm}(x) + C_{\mp}(x) e^{\mp 2i \int_{x_0}^x dx' p(x')} \right] \quad (40)$$

From the boundary conditions in Eqs. (29) and (30), we have

$$C_+(-\infty) = 0, \quad (41)$$

$$C_-(\infty) = (E^2 - m^2)^{1/4} e^{-i\sqrt{E^2 - m^2} x_0} e^{i \int_{x_0}^{\infty} dx' (\sqrt{E^2 - V(x')} - \sqrt{E^2 - m^2})}. \quad (42)$$

Finally, with these boundary values, the differential equations in Eq. (40) can be turned into integral equations,

$$C_+(x) = -i \int_{-\infty}^x dx' \left(\frac{p''(x')}{4p(x')^2} - \frac{3(p'(x'))^2}{8p(x')^3} \right) \left[C_+(x') + C_-(x') e^{-2i \int_{x_0}^{x'} dx'' p(x'')} \right], \quad (43)$$

$$C_-(x) = C_-(\infty) - i \int_{x'}^{\infty} dx' \left(\frac{p''(x')}{4p(x')^2} - \frac{3(p'(x'))^2}{8p(x')^3} \right) \left[C_-(x') + C_+(x') e^{2i \int_{x_0}^{x'} dx'' p(x'')} \right]. \quad (44)$$

To the lowest order, we just substitute the boundary values of C_{\pm} into the right hand side of the above equations,

$$C_+(x) \approx -i C_-(\infty) \int_{-\infty}^x dx' \left(\frac{p''(x')}{4p(x')^2} - \frac{3(p'(x'))^2}{8p(x')^3} \right) e^{-2i \int_{x_0}^{x'} dx'' p(x'')}, \quad (45)$$

$$C_-(x) \approx C_-(\infty) \left[1 - i \int_{x'}^{\infty} dx' \left(\frac{p''(x')}{4p(x')^2} - \frac{3(p'(x'))^2}{8p(x')^3} \right) \right]. \quad (46)$$

Under this approximation, the reflection coefficient becomes

$$R = \frac{C_+(\infty)}{(E^2 - m^2)^{1/4}} e^{-i\sqrt{E^2 - m^2} x_0} e^{i \int_{x_0}^{\infty} dx' (\sqrt{E^2 - V(x')} - \sqrt{E^2 - m^2})}, \quad (47)$$

with

$$C_+(\infty) = -i C_-(\infty) \int_{-\infty}^{\infty} dx' \left(\frac{p''(x')}{4p(x')^2} - \frac{3(p'(x'))^2}{8p(x')^3} \right) e^{-2i \int_{x_0}^{x'} dx'' p(x'')}, \quad (48)$$

as given in Eq. (45). The reflection probability in this approximation becomes

$$\begin{aligned} \mathcal{R} &= |R|^2 \\ &= \left| \int_{-\infty}^{\infty} dx' \left(\frac{p''(x')}{4p(x')^2} - \frac{3(p'(x'))^2}{8p(x')^3} \right) e^{-2i \int_{x_0}^{x'} dx'' p(x'')} \right|^2, \end{aligned} \quad (49)$$

while the transmission coefficient is given by

$$\begin{aligned} \mathcal{T} &= 1 - \mathcal{R} \\ &= 1 - \left| \int_{-\infty}^{\infty} dx' \left(\frac{p''(x')}{4p(x')^2} - \frac{3(p'(x'))^2}{8p(x')^3} \right) e^{-2i \int_{x_0}^{x'} dx'' p(x'')} \right|^2. \end{aligned} \quad (50)$$

This constitutes our WKB approximation for $E^2 \gg V_m$ as long as the validity condition in Eq. (34) is satisfied. Note that we can also obtain, in this approximation, the wavefunction by substituting $C_+(x)$ and $C_-(x)$ in Eqs. (45) and (46), respectively, into Eq. (38).

B. $E^2 \approx V_m$

In the case of a potential barrier, when the energy E of the field is decreased to such an extent that E^2 is close to the peak of the potential, the validity condition (Eq. (34)) will no longer be satisfied near x_m , the position of the peak. This situation can be remedied by representing the part of the potential near x_m as a parabola, while maintaining the WKB solutions on either side of it. Exact solutions can be found for the parabolic potential, and then the approximate solution for the whole range, $-\infty < x < \infty$, can be obtained by matching the three solutions across the intertwining regions [5, 6].

For the part of the potential near x_m , we can write, in the parabolic approximation,

$$V(x) \approx V_m + \frac{1}{2}V''(x_m)(x - x_m)^2, \quad (51)$$

and

$$\begin{aligned} E^2 - V(x) &\approx (E^2 - V_m) + \lambda(x - x_m)^2 \\ &\approx \begin{cases} \sqrt{\lambda}(z^2 + \xi^2) & E^2 > V_m \\ \sqrt{\lambda}(z^2 - \xi^2) & E^2 < V_m \end{cases} \end{aligned} \quad (52)$$

where

$$\lambda = -V''(x_m)/2, \quad z = \lambda^{1/4}(x - x_m), \quad \text{and} \quad \xi = \frac{|E^2 - V_m|^{1/2}}{\lambda^{1/4}}. \quad (53)$$

Note that for

$$z = \pm\xi \Rightarrow x_{1,2} = x_m \pm \frac{|E^2 - V_m|^{1/2}}{\sqrt{\lambda}}. \quad (54)$$

When E^2 is smaller than V_m , x_1 and x_2 are just the turning points with $E^2 = V(x_{1,2})$. In any case for $E^2 \approx V_m$, we can divide x into three regions: (I) $x > x_1$, (II) $x_1 > x > x_2$, and (III) $x < x_2$. For regions (I) and (III), we still use the WKB form of the wavefunction,

$$\begin{aligned} \psi_I(x) &= A_+W_+(x) + A_-W_-(x), \\ \psi_{III}(x) &= BW_+(x). \end{aligned} \quad (55)$$

For region II, we have, in the parabolic approximation, the Schrödinger equation in Eq. (38) can be written as

$$\frac{d^2\psi}{dz^2} + (z^2 \pm \xi^2)\psi = 0, \quad (56)$$

with the general solution

$$\psi_{II}(z) = \alpha D_{-\frac{1}{2} \mp \frac{i\xi^2}{2}}(\sqrt{2}e^{i\pi/4}z) + \beta D_{-\frac{1}{2} \mp \frac{i\xi^2}{2}}(-\sqrt{2}e^{i\pi/4}z), \quad (57)$$

where $D_\nu(t)$ are the parabolic cylinder functions.

Taking into account of the boundary conditions in Eqs. (29) and (30), and matching the wavefunctions in different regions across $x = x_1$ and x_2 , we can solve for the constants A_+ , A_- , α , β , and B [6, 8]. One can then obtain

$$\mathcal{T} = \begin{cases} 1/(1 + e^{-\pi\xi^2}) & E^2 > V_m \\ 1/(1 + e^{\pi\xi^2}) & E^2 < V_m \end{cases} \quad (58)$$

These two cases can be combined by writing

$$\mathcal{T} = \frac{1}{1 + e^{\pi(V_m - E^2)/\sqrt{\lambda}}}, \quad (59)$$

which is the WKB approximation we shall use for $E^2 \approx V_m$.

C. $E^2 \ll V_m$

When the energy E of the field is lowered further, the turning points x_1 and x_2 will move far apart in such a way that the parabolic approximation is no longer valid. In this case, one can divide the x -axis into five regions: (I) $x > x_1$, (II) $x \approx x_1$, (III) $x_1 > x > x_2$, (IV) $x \approx x_2$, and (V) $x < x_2$. For regions (I), (III), and (V), we still use the standard WKB wavefunctions,

$$\begin{aligned} \psi_I(x) &= A_+ W_+(x) + A_- W_-(x), \\ \psi_{III}(x) &= B_+ W_+(x) + B_- W_-(x), \\ \psi_V(x) &= C W_+(x). \end{aligned} \quad (60)$$

For region (II), we use the linear approximation [6],

$$V(x) \approx V(x_1) + V'(x_1)(x - x_1), \quad (61)$$

and

$$E^2 - V(x) \approx \mu_1^{2/3} z_1, \quad (62)$$

where

$$\mu_1 = -V'(x_1), \quad \text{and} \quad z_1 = \mu_1^{1/3}(x - x_1). \quad (63)$$

Then the Schrödinger equation becomes

$$\frac{d^2\psi}{dz_1^2} + z_1\psi = 0, \quad (64)$$

with the general solution

$$\psi_{II}(z_1) = \alpha \text{Ai}(-z_1) + \beta \text{Bi}(-z_1), \quad (65)$$

where $\text{Ai}(t)$ and $\text{Bi}(t)$ are Airy functions. One can consider region (IV) in a similar way to obtain

$$\psi_{IV}(z_2) = \gamma \text{Ai}(z_2) + \delta \text{Bi}(z_2), \quad (66)$$

where

$$\mu_2 = -V'(x_2), \quad \text{and} \quad z_2 = \mu_2^{1/3}(x - x_2). \quad (67)$$

Again matching the boundary conditions at $x = \pm\infty$ and the wavefunctions across $x = x_1$ and x_2 , one can obtain the constants A_+ , A_- , B_+ , B_- , C , α , β , γ , and δ . The transmission probability is then given by

$$\mathcal{T} = e^{-2 \int_{x_2}^{x_1} dx' \sqrt{V(x') - E^2}}. \quad (68)$$

This is our WKB approximation for the cases with $E^2 \ll V_m$.

IV. TRANSMISSION PROBABILITIES FOR THE DIRAC FIELD

Using the WKB approximations outlined above we shall calculate in this section the transmission probabilities for the Dirac field in the radial equation (Eq. (14)) with the potential as given by Eq. (24).

A. Massless cases

First, we consider the massless cases, with the potential

$$V(r, \kappa) = \frac{|\kappa| \Delta^{1/2}}{r^4} [|\kappa| \Delta^{1/2} - (r - 3)], \quad (69)$$

where we have used the mass M of the black hole as a unit of mass and length to simplify the notation so that $\Delta = r(r - 2)$. To proceed we first consider the case with $\kappa = 1$. Then we have

$$\sqrt{V_m} = 0.216. \quad (70)$$

Hence, for $E \gg 0.216$, we can use the formula in Eq. (50) to evaluate the transmission probability. To check the validity condition, we plot $|V'/2p^3|$ for various energy E in Fig. 3.

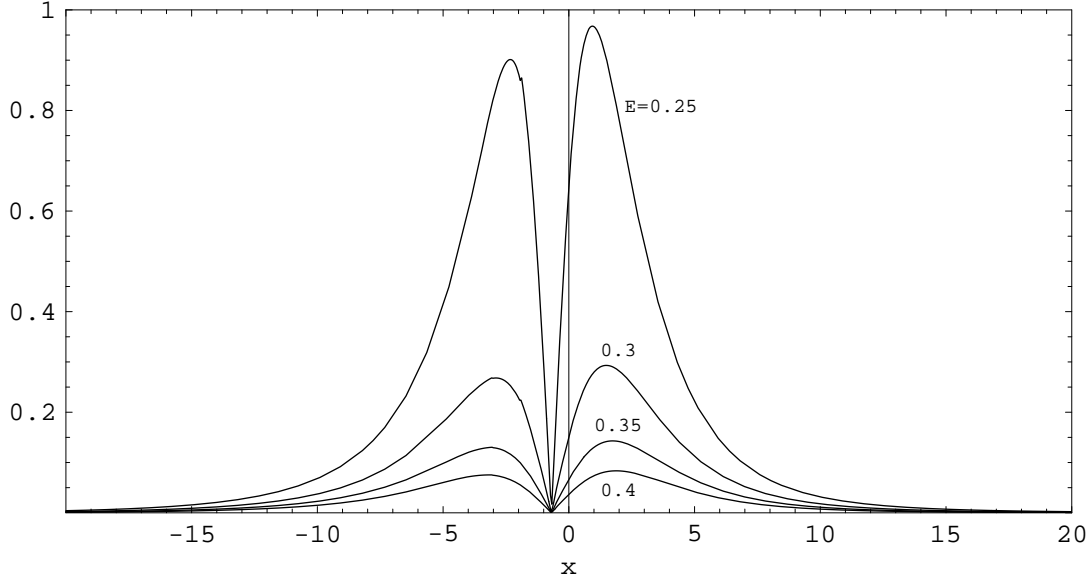


FIG. 3: Validity condition for various values of E of the massless Dirac fields with $\kappa = 1$.

From it, we see that for $E = 0.35$, the maximum value of this quantity,

$$\left| \frac{V'}{2p^3} \right|_{max} \approx 0.1. \quad (71)$$

The formula in Eq. (50) can therefore be a good approximation for energy E larger than around 0.35. The transmission probabilities \mathcal{T} for $0.35 \leq E \leq 1$ calculated from this formula is plotted in Fig. 4.

For E smaller than 0.35, one can use the parabolic approximation for the transmission probability as given in Eq. (59). The transmission probabilities for $0 \leq E \leq 0.35$ calculated from this approximation is also plotted in Fig. 4. Near the base of the barrier, the parabolic approximation is no longer valid because the turning points are far apart. This is apparent from the fact that the curve tends to around 0.0377 instead of zero as E goes to zero.

When the turning points are isolated, one can use the approximation given in Eq. (68) for the transmission probability \mathcal{T} . The transmission probabilities for $0 \leq E \leq 0.216$ calculated from Eq. (59) are also plotted in Fig. 4. When E is close to $\sqrt{V_m} = 0.216$, the formula in Eq. (59) cannot be trusted as we can see that $\mathcal{T} \rightarrow 1$ as $E \rightarrow V_m$ in this approximation.

In Fig. 4, we see that the solid and dashed lines calculated from these two approximations overlap at around $E = 0.154$. Thus for $E > 0.154$, we should take the result with the parabolic approximation (solid line) and for $E < 0.154$, we should take that of the tunneling approximation (dashed line) instead. While in the region with $E \approx 0.154$, we can extrapolate

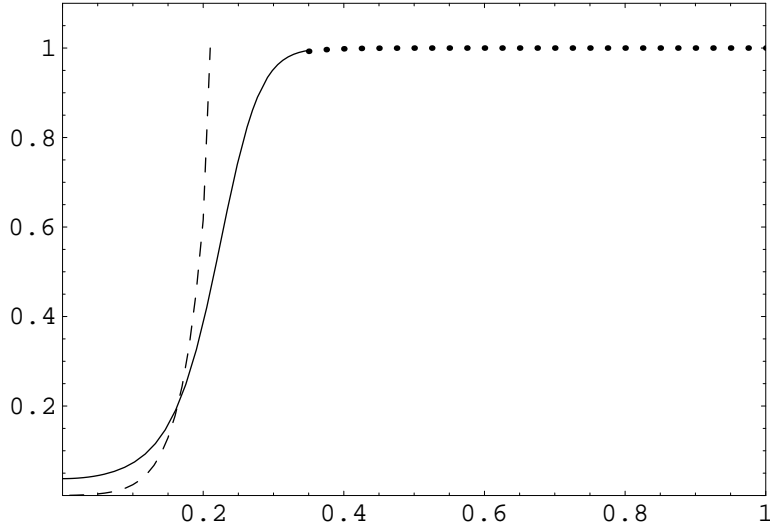


FIG. 4: Transmission probabilities of the massless Dirac field with $\kappa = 1$ in the various WKB approximations for $E^2 \gg V_m$ (dotted line), $E^2 \approx V_m$ (solid line), and $E^2 \ll V_m$ (dashed line).

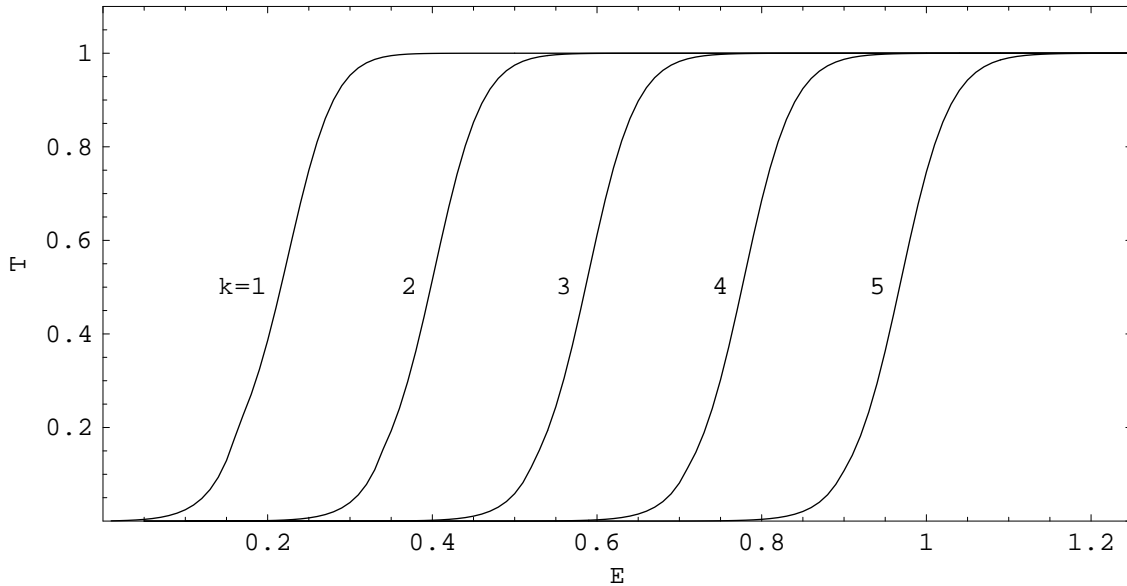


FIG. 5: Transmission probabilities \mathcal{T} of the massless Dirac field with $\kappa = 1$ to 5.

smoothly between these two curves. Combining with the result for $E > 0.35$, we can obtain a curve for the transmission probabilities in the entire region, $0 < E < 1$. This is plotted in Fig. 5.

In addition to the curve for $\kappa = 1$, we also plot the transmission probabilities for $\kappa = 2, 3, 4$, and 5 in Fig. 5. These curves are obtained in the same procedure as outlined above

for $\kappa = 1$. They are similar to each other and shift to the right as κ increases. The energy at which $\mathcal{T} = 1/2$ occurs is $\sqrt{V_m}$ which increases as the peak of the barrier gets higher and higher when κ is increased.

B. Massive cases

The situations with nonzero m are more complicated because the potentials can change from a barrier to a step or vice versa as the parameters m and κ are varied as shown in Figs. 1 and 2. With $\kappa = 1$, the potentials are barriers for $m = 0, 0.1, \text{ and } 0.2$. One can use the relevant approximations for different values of the energy E , along the same lines as in the massless cases in the last subsection. The results are plotted in Fig. 6. However, for $m = 0.3, 0.4, \text{ and } 0.5$, the potentials are steps. The only approximation one needs is for $E \gg m$. We also check the validity condition and the result indicates that the approximation is useful all the way down to energy value very close to m . The results for these masses are also plotted in Fig. 6. For the potential steps, the transmission probabilities are almost equal to 1, which are consistent with the classical results.

We also see from the various diagrams in Fig. 6 that the variations of the transmission probabilities \mathcal{T} with m are numerically very small. In order to see the changes in more details, we plotted \mathcal{T} versus m in Fig. 7 for $E = 1$ and $\kappa = 1$. Since the transmission probabilities in these cases are very close to 1, we take the logarithmic of \mathcal{T} in the plot. From this figure we see that \mathcal{T} first decreases from $m = 0$, attends a minimum around $m = 0.14$, and then increases as m is further increased.

The variations of \mathcal{T} between $m = 0.3$ to 0.5 are quite unexpected. This is because with these values of m , the potentials are in the form of steps with larger and larger step height when m is increased. For simple potential steps, it is known that the transmission probabilities decrease as the steps get higher and higher for fixed energy. We thus see that for the black hole effective potentials, the transmission probabilities are not determined only by the height of the potential but also the overall shape of it.

In Fig. 7, $E = 1$ and is much larger than $\sqrt{V_m}$. For energy values closer to $\sqrt{V_m}$, the variations can be quite different. As shown in Fig. 8, for $E = 0.2$, that is, when E^2 is near the peak of the potential, \mathcal{T} increases first as m is increased from 0, attends a maximum value around $m = 0.09$, and then decreases. The same trend is found for $E = 0.1$ where it is

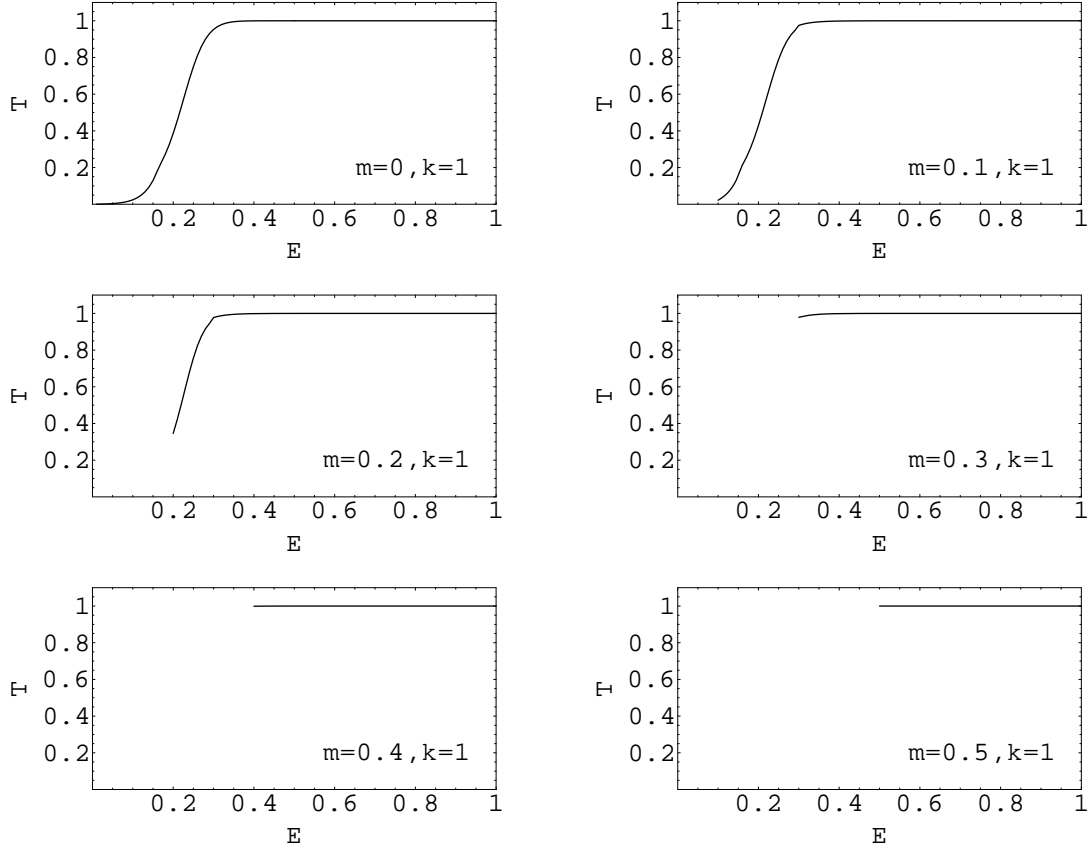


FIG. 6: Transmission probabilities \mathcal{T} of the Dirac field with $\kappa = 1$ and $m = 0$ to 0.5 .

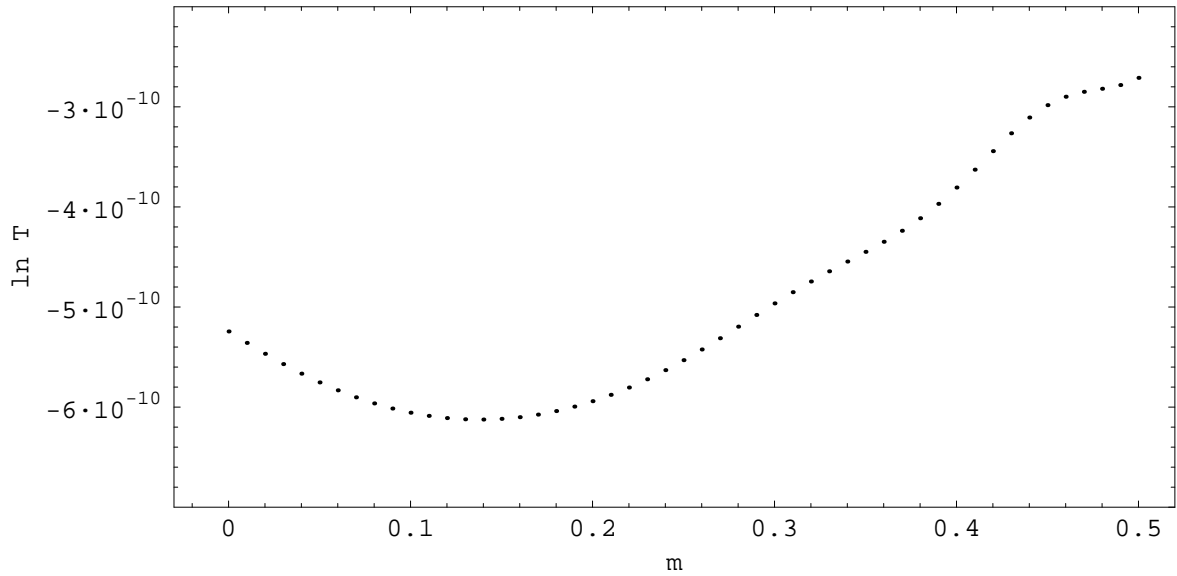


FIG. 7: Variation of the logarithmic of the transmission probabilities of the Dirac field ($E = 1$ and $\kappa = 1$) with m .

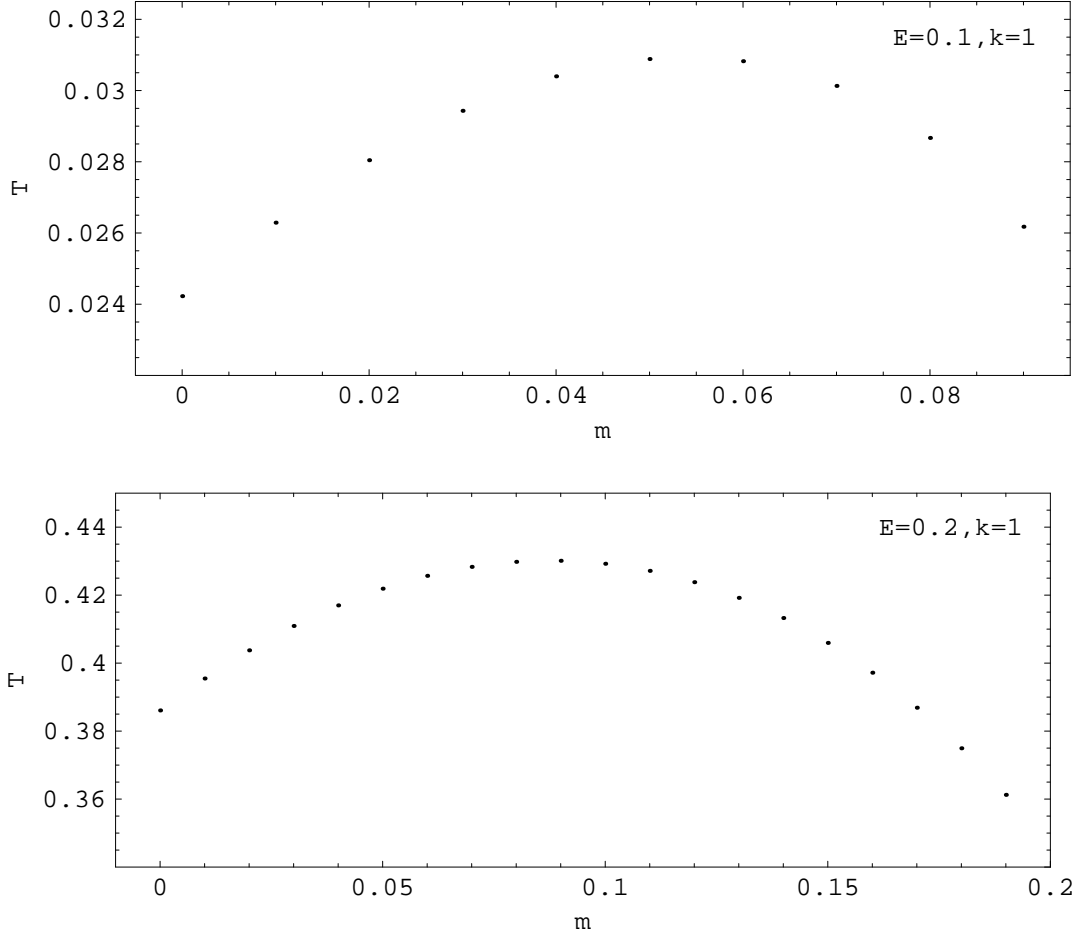


FIG. 8: Variation of the transmission probabilities of the Dirac field with m for $E = 0.1$ and 0.2 .

well below the peak of the potential. However, the maximum value in this case is at around $m = 0.05$.

As we can see from the above discussions, the transmission probability \mathcal{T} in general increases with the mass m when m is large enough that the effective potential is in the form of a step. However, when m is smaller and the effective potential is in the form of a barrier, the variations of \mathcal{T} with m can be quite complicated. When E is large and well above the peak, \mathcal{T} first decreases and then increases when m is increased from $m = 0$. When E is small with its value near or well below the peak of the potential, the variation is reversed, that is, \mathcal{T} first increases and then decreases when m is increased from $m = 0$.

V. CONCLUSIONS AND DISCUSSIONS

We study the radial equations of the massive Dirac field in the spherically symmetric Schwarzschild spacetime. Using the WKB approximations and the appropriate connection formulae, we are able to give semianalytic formulae for the transmission probability \mathcal{T} of the radial wavefunction with the energy $E^2 \gg V_m$, $E^2 \approx V_m$, and $E^2 \ll V_m$, V_m is the maximum value of the effective potential. For the massless cases, we find that, as shown in Fig. 5, the variations of \mathcal{T} with the energy E and the angular momentum number κ are similar to that for the scalar case [1, 17]. Since the potentials are in the form of barriers and the heights of the peaks of these barriers increase with κ , \mathcal{T} for fixed E will thus decrease as expected. This means that waves with lower angular momenta but with fixed energy will be absorbed more easily by the black hole.

The massive cases are more complicated. The effective potentials in these cases change from barriers to steps when the mass of the field is increased. When the potential is still in the form of a step and the energy E of the field is well above the maximum value of the potential, the transmission probability \mathcal{T} decreases with m . Thus higher mass fields will get absorbed by the black hole more easily. However, when m is decreased to such an extent that the potentials become barriers, the variation trend changes as shown in Fig. 7. At some value of m (around 0.14 for $E = 1$ and $\kappa = 1$), \mathcal{T} turns around and increases when m is further decreased to 0. Therefore, we see that the variations of \mathcal{T} with m is complicated when the potentials are in the form of barriers. This is also true when E is smaller with its value near or well below the peak of the potential as shown in Fig. 8.

After calculating the transmission probabilities for the radial wavefunctions, one can evaluate the corresponding phase shifts and cross sections in various scattering situations [1]. In the semiclassical limit one can also study the interesting phenomena such as black hole glories [18], orbiting and spiraling scatterings [19] by deriving the semiclassical deflection function [20]. We hope to further investigate these issues in our future publications.

Quite peculiarly for black holes, one can also study the absorption cross sections for various wave fields. There has been quite a lot of interest in these cross sections in relation to the higher-dimensional black holes in string theory, especially the low-energy absorption cross sections [21]. However, the WKB approximations that we use in this work is not adequate at low energy, that is, when $E \approx m$. One can nevertheless improve the WKB

approximations in these threshold situations when E is near the top of the step or when it is near the base of the barrier [22, 23]. This improved approximations may therefore provide an alternative to the usual method [3] in obtaining these low-energy absorption cross sections.

Acknowledgments

This work is supported by the National Science Council of the Republic of China under contract number NSC 91-2112-M-032-011.

-
- [1] J. A. H. Futterman, F. A. Handler, and R. A. Matzner, *Scattering from Black Holes* (Cambridge University Press, 1988).
 - [2] J. Hough and S. Rowen, *Living Rev. Relativity* **3**, 3 (2000).
 - [3] W. G. Unruh, *Phys. Rev. D.* **14**, 3251 (1976).
 - [4] F. Finster, J. Smoller, and S.-T. Yau, *J. Math. Phys.* **41**, 3943 (2000).
 - [5] M. V. Berry and K. E. Mount, *Rept. Prog. Phys.* **35**, 315 (1972).
 - [6] C. M. Bender and S. A. Orszag, *Advanced Mathematical Methods for Scientists and Engineers* (McGraw Hill, 1978).
 - [7] B. F. Schutz and C. M. Will, *Astrophys. J. Lett.* **291**, L33 (1985).
 - [8] S. Iyer and C. M. Will, *Phys. Rev. D.* **35**, 3621 (1987).
 - [9] B. Mukhopadhyay and S. K. Chakrabarti, *Class. Quantum Grav.* **16**, 3165 (1999).
 - [10] H. T. Cho, *Phys. Rev. D.* **68**, 024003 (2003).
 - [11] D. R. Brill and J. A. Wheeler, *Rev. Mod. Phys.* **29**, 465 (1957).
 - [12] P. B. Groves, P. R. Anderson, and E. D. Carlson, *Phys. Rev. D.* **66**, 124017 (2002).
 - [13] J. D. Bjorken and S. D. Drell, *Relativistic Quantum Mechanics* (McGraw Hill, 1964).
 - [14] S. Chandrasekhar, *The Mathematical Theory of Black Holes* (Clarendon Press, 1983).
 - [15] F. Cooper, A. Khare, and U. Sukhatme, *Phys. Rept.* **251**, 267 (1995).
 - [16] A. Anderson and R. H. Price, *Phys. Rev. D.* **43**, 3147 (1991).
 - [17] N. Sanchez, *Phys. Rev. D.* **18**, 1030 (1978).
 - [18] R. A. Matzner, C. DeWitt-Morette, B. L. Nelson, and T.-R. Zhang, *Phys. Rev. D.* **31**, 1869 (1985).

- [19] P. Anninos, C. DeWitt-Morette, P. Yioutas, and T. R. Zhang, *Phys. Rev. D.* **46**, 4477 (1992).
- [20] K. W. Ford and J. A. Wheeler, *Ann. Phys.* **7**, 259 (1959).
- [21] S. R. Das, G. Gibbons, and S. D. Mathur, *Phys. Rev. Lett.* **78**, 417 (1997).
- [22] C. Eltschka, H. Friedrich, M. J. Moritz, and J. Trost, *Phys. Rev. A.* **58**, 856 (1998).
- [23] M. J. Moritz, *Phys. Rev. A.* **60**, 832 (1999).